PHYSICAL REVIEW VOLUME 106, NUMBER 4 MAY 15, 1957

# Paramagnetic Effect in Superconductors: IV. Measurements on Aluminum*†

A. H. FITCH‡ AND HANS MEISSNER
*Department of Physics, The Johns Hopkins University, Baltimore, Maryland*
(Received February 11, 1957)

A cryostat has been designed and constructed to permit investigation of superconductors having transition temperatures in the range from 1.4°K to below 0.9°K. By means of this cryostat, the paramagnetic effect, previously observed in In, Sn, Ta, Hg, Tl, and NbN, has been observed at the superconducting transition of aluminum. The threshold current, $I_0$, required for the occurrence of the paramagnetic effect, had previously been shown to be related to the applied longitudinal field, $H_{z0}$, and the specimen diameter, $d$, by the equation

$$I_0=I_g+\gamma^*\pi H_{z0}d,$$

where $I_g$ and $\gamma^*$ are constants characteristic of a particular superconductor. Preliminary measurements on the six superconductors listed above had suggested that $I_g$ values occur only in multiples of 0.6 ampere. Measurements of $I_g$ for aluminum yield an $I_g$ value definitely less than 0.6 amp.

## I. INTRODUCTION

WHEN a cylindrical current-carrying superconductor is cooled through its transition temperature in the presence of a longitudinal magnetic field, the magnetic flux in the specimen may show an increase over the value which it had in the normal state. This apparent increase in the permeability, which is referred to as the paramagnetic effect, has been investigated[1–6] in a number of superconductors since its discovery in tin by Steiner and Schoeneck.[1] It has been established that a threshold current, $I_0$, exists below which the effect does not occur. $I_0$ is given by

$$I_0=I_g+\gamma^*\pi H_{z0}d,$$

TABLE I. Summary of the $I_g$ and $\gamma^*$ values.

| Element | $I_g$ amp | $\gamma^*$ | Reference |
|---|---|---|---|
| Tin | 1.6±0.7 | 0.83±0.04 | Thompson[a] |
| | 1.2 | 0.67 | Steiner[b] |
| | 1.2 | 0.91 | Shibuya and Tanuma[c] |
| Indium | 0.3±0.2 | 0.83±0.04 | Thompson[a] |
| | 0.2±0.3 | 0.83±0.04 | Thompson[a] |
| | 0.6 | 0.67 | Steiner[b] |
| Thallium | 0.9±0.3 | 0.83±0.04 | Thompson[a] |
| | 0.6 | 0.37 | Steiner[b] |
| Mercury | 1.7 | 0.37 | Meissner *et al.*[d] |
| Tantalum | 0.6 | ··· | Meissner *et al.*[d] |
| Niobium nitride[f] | 2.35 | 0.67 | Sellmaier[e] |
| Aluminum | 0.3±0.2 | 1.0 | Present work |

[a] See reference 5.
[b] See reference 2.
[c] See reference 4.
[d] See reference 3.
[e] See reference 6.
[f] These data were found for a hollow NbN cylinder on a Nb core; all other data were obtained for solid cylinders.

where $I_g$ and $\gamma^*$ are constants for a particular superconductor, $H_{z0}$ is the applied longitudinal magnetic field, and $d$ is the specimen diameter. Table I summarizes all of the superconductors for which either $I_g$ or $\gamma^*$ has been measured to date.

Of the superconducting elements for which the paramagnetic effect has not yet been observed, only vanadium, lead, and niobium have transition temperatures in the temperature range 4.2°K to 10°K. Against this, aluminum, zinc, gallium, rhenium, and thorium have transition temperatures in the range 1.39°K to 0.9°K. Because of this, it was decided to build a cryostat which could operate down to temperatures of 0.9°K. This investigation on aluminum represents the first in a series on the latter group of superconductors.

## II. EXPERIMENTAL ARRANGEMENT

### (a) Cryostat

The cryostat used in this investigation is of the type in which the temperature is reduced by pumping through a small orifice over an adiabatically isolated bath of liquid helium. The thermal isolation is accomplished by a vacuum jacket whose outside wall is maintained at 4.2°K. Several cryostats which employ this method have been described in the literature.[7–14] The more recent of these employ high pumping speeds (600–1000 liters/sec) and are able to cool a considerably larger volume than the early designs. Figure 1 shows the general plan of the cryostat used in this investigation. The inner bath is pumped by a C.V.C. MB-200 oil booster pump which is backed by a Leybold mercury booster pump Hg-45 and a Kinney rotary pump

* Supported by a grant of the National Science Foundation.
† Part of a dissertation (A.H.F.) submitted to the Physics Department of The Johns Hopkins University in partial fulfillment of the requirements for the degree of Doctor of Philosophy.
‡ Union Carbide and Carbon Fellow 1954–1955; present address: Bell Telephone Laboratories, Whippany, New Jersey.
[1] K. Steiner and H. Schoeneck, Physik. Z. 44, 346 (1943).
[2] K. Steiner, Z. Naturforsch. 49, 271 (1949).
[3] Meissner, Schmeissner, and Meissner, Z. Physik 130, 521 (1951); 130, 529 (1951); 132, 529 (1952).
[4] Y. Shibuya and S. Tanuma, Phys. Rev. 98, 938 (1955).
[5] J. C. Thompson, Phys. Rev. 102, 1004 (1956).
[6] A. Sellmaier, Z. Physik 141, 550 (1955).
[7] H. Kamerlingh Onnes, Trans. Faraday Soc. 18, 53 (1922).
[8] W. H. Keesom, Proc. Roy. Acad. Amsterdam 35, 136 (1932).
[9] A. H. Cooke and R. A. Hull, Nature 143, 799 (1939).
[10] B. G. Lasarew and B. N. Eselson, J. Phys. U.S.S.R. 5, 151 (1941).
[11] B. N. Eselson, J. Exptl. Theoret Phys. (U.S.S.R.) 18, 799 (1948).
[12] Atkins, Edwards, and Pullan, Rev. Sci. Instr. 26, 49 (1955).
[13] Kilpatrick, Hammel, and Mapother, Phys. Rev. 97, 1634 (1955).
[14] Cochran, Mapother, and Mould, Phys. Rev. 103, 1657 (1956).

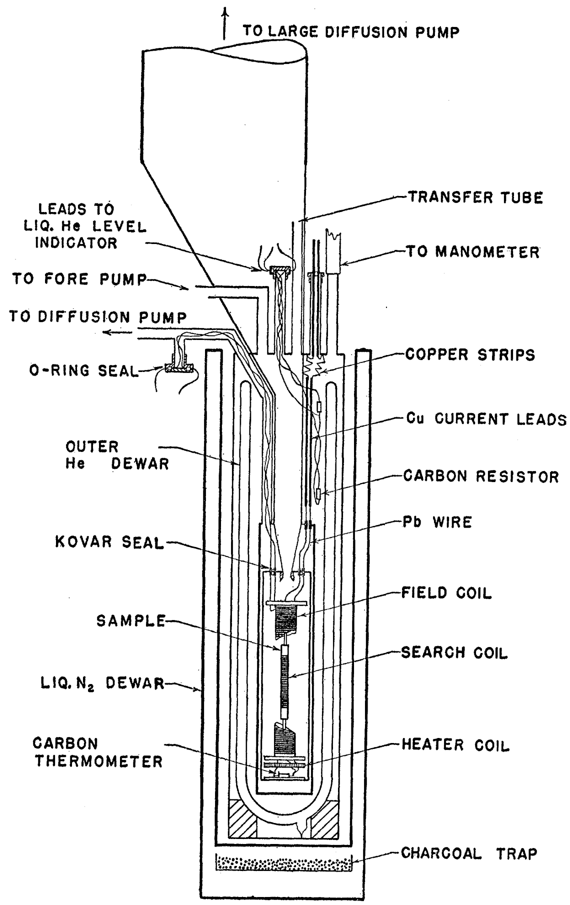


FIG. 1. Cryostat for production of temperatures in the range 0.8°K to 1.3°K.

VSM-556. Selection of a series of pumps, such as those used in this application, is greatly facilitated by a diagram such as Fig. 2. The throughput of all three pumps in mm Hg×liters/sec is plotted *versus* the pressure in mm Hg. The MB-200 has a limiting forepressure of 0.6-mm Hg at which it is removing a quantity of gas of 8-mm Hg×liters/sec. From the diagram, it can be seen that neither the Hg-45 nor the MB-200 can handle throughputs greater than 8-mm Hg×liters/sec and, in practice, it is advisable to operate at throughputs at least a factor of two below this figure. Neglecting film flow, this throughput corresponds to a heat input to the inner liquid helium vessel of $1.5\times10^{-2}$ watt.—The vacuum jacket is continuously pumped with a C.V.C. MCF-60 oil diffusion pump.

The conical orifice to the inner liquid helium vessel is made of German silver and has a limiting throat diameter of 7 mm. In choosing the orifice diameter, one must find a compromise between the excessive film flow allowed by a large diameter orifice and the excessive reduction of conductance by a small diameter. The 7-mm throat represents this compromise.

The conductance increases approximately as the cube of the throat diameter, whereas the film flow increases only as the first power. The ratio of film flow to total flow is therefore smaller for systems having pumps of higher speeds, provided that the proper choice of orifice diameter has been made for the pump in question. For the MB-200 and heat inputs of $10^{-3}$ watt, the above ratio is less than 0.1.

The ducts leading to the orifice are of a conical construction to avoid the turbulence which would appear at sharp edges or bends. The increase in diameter of the cones was chosen so as to approximately match the expansion which the temperature change produces in the emerging vapor. The upper cones were constructed from 0.25-mm sheet supernickel, while the lowest one was machined from German silver rod. With the exception of the outer liquid helium Dewar which was Pyrex, all of the cylindrical vessels were made of brass.

The high-current connections were brought from room temperature to the 4.2°K liquid helium bath by a method previously described.[15] From there the specimen current was carried by lead (Pb) wires which were brought into both the vacuum jacket and the inner vessel through Kovar seals. Since lead is superconducting below 7.2°K these leads contribute no Joule heating in the low-temperature bath.

All other connections were of No. 40 wire, with manganin used wherever possible. These leads were brought from a seal at room temperature through a tube into the vacuum jacket where they were clamped at 4.2°K. From there they led through Kovar terminals into the inner vessel.

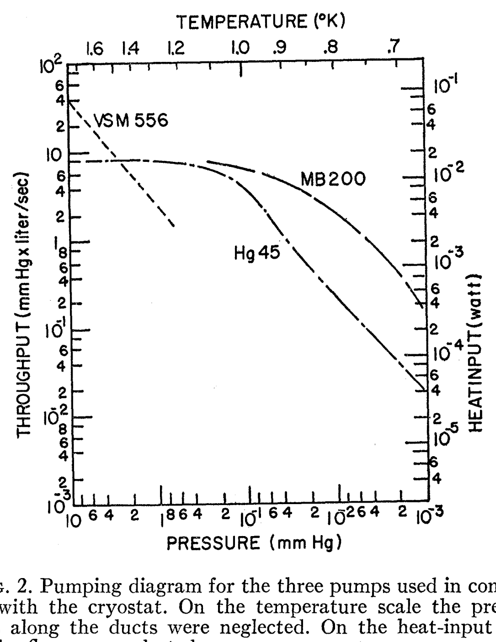


FIG. 2. Pumping diagram for the three pumps used in conjunction with the cryostat. On the temperature scale the pressure drops along the ducts were neglected. On the heat-input scale the film flow was neglected.

[15] H. Meissner, Phys. Rev. **101**, 1660 (1956).

### (b) Operating Procedure

Prior to a run, the system is first precooled with liquid nitrogen. The liquid nitrogen is then removed and the transfer of liquid helium into the Pyrex Dewar is started. As soon as the liquid begins to collect, helium gas at a pressure greater than one atmosphere is introduced into the inner vessel through a counterflow heat exchanger, not shown in Fig. 1. This helium almost immediately begins to condense in the inner vessel. In order to effect a more rapid cooling of the inner vessel and its contents, the vacuum jacket is filled with helium gas at a pressure of a few mm Hg. Usually, the inner vessel is filled with condensed helium by the time the Pyrex Dewar is full; both liquid levels are measured by means of carbon resistance thermometers. The exchange gas is then pumped out of the vacuum jacket in preparation for cooling down to the transition temperature of aluminum. Since the pumping speed of the Hg-45 is effectively zero at pressures above 10 mm Hg, the system is first roughed down to this limiting forepressure with the VSM 556. During this roughing period, several calibration points are obtained for the carbon resistance thermometer by simultaneously measuring the helium vapor pressure with a U-tube manometer and the thermometer resistance with a Wheatstone bridge. When the transition temperature of the sample is reached, the regulating valves on the pumping system are adjusted to maintain the temperature approximately constant. The fine-temperature regulation is accomplished by manually varying the current to a 1-ohm manganin heater coil in the inner vessel. To reach the transition temperature of aluminum, it was not necessary to use the MB-200, this pump having been installed for investigations at lower temperatures.

### (c) Specimens and Measuring Equipment

Three specimens were used in this investigation, and they were all prepared from 99.99% pure ingots supplied by the Aluminum Company of America.[16] The first specimen, hereafter referred to as Al I, was a polycrystalline cylinder 69.6 mm long and 5 mm in diameter, which was annealed for 24 hours in vacuum prior to use. The second and third specimens, Al II and Al III, were single crystal cylinders of diameters 3.1 mm and 6.0 mm respectively. These were vacuum melted and grown in crucibles of high-purity A.E.C. graphite. All three specimens were etched and electrolytically polished. The following residual resistance ratios, $r_0 = R_{1.2^\circ K}/R_{273^\circ K}$, were obtained for the three specimens: Al I, $r_0=0.62\times10^{-3}$; Al II, $r_0=0.86\times10^{-3}$; Al III, $r_0=2.43\times10^{-3}$.

Figure 1 shows the general arrangement of sample, search coil, and field coil used in the present work. In addition, two potential clips, not shown in Fig. 1, were attached to the sample for resistance measurements. The search coil, used for detecting the change in flux, was wound directly onto the specimen and was connected to a Leeds and Northrup ballistic galvanometer, type 2284 b, having a coil resistance of 17 ohms, a period of 7.4 sec, an external critical damping resistance of 17 ohms, and a ballistic sensitivity of $2\times10^{-8}$ v sec/mm at a scale distance of 5 m.

The longitudinal magnetic field, $H_{z0}$, was produced by a field coil surrounding the specimen (see Fig. 1). The field coil was wound with 88.4 turns/cm of tantalum wire. Since the tantalum wire becomes superconducting at 4.4°K, the field coil itself produces no Joule heating in the inner liquid helium vessel. Both the horizontal and vertical components of the earth's magnetic field were compensated by a set of Helmholtz coils, not shown in Fig. 1.

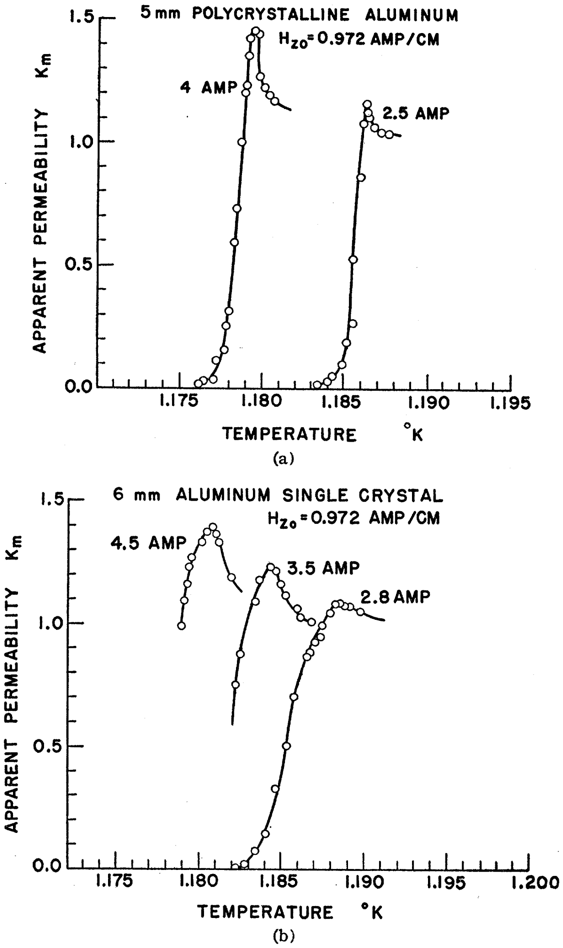


FIG. 3. (a) $K_m$ *vs* $T$ curves for the 5-mm-diameter polycrystalline aluminum specimen (Al I). (b) $K_m$ *vs* $T$ curves for the 6-mm-diameter aluminum single crystal (Al III).

### III. MEASUREMENTS

When recording the data, the procedure was slowly to vary the current to the manganin heater coil, which

[16] We desire to express our thanks to the company for supplying the aluminum free of charge.

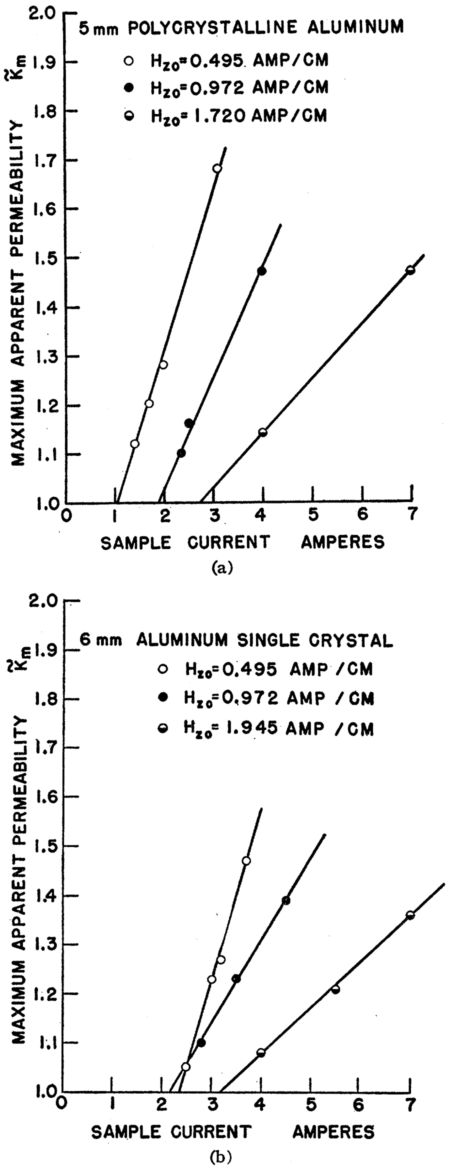


FIG. 4. (a) $\tilde{K}_m$ *vs* $I$ curves for the 5-mm-diameter polycrystalline aluminum specimen (Al I). (b) $\tilde{K}_m$ *vs* $I$ curves for the 6-mm-diameter aluminum single crystal (Al III).

thereby changed the thermometer readings from point to point through the transition while holding the current fixed. At each fixed temperature, the applied magnetic field was reversed and the resulting galvanometer deflection, $\alpha$, recorded. The carbon thermometer readings were converted to temperature by means of the two-constant formula given by Clement.[17] The galvanometer deflections, $\alpha$, were converted to apparent permeability, $K_m$, through the equation

$$K_m = (\alpha - \alpha_{00})/(\alpha_0 - \alpha_{00}).$$

Here, $\alpha_0$ is the deflection produced upon reversing the field, $H_{z0}$, when the specimen is in the normal state; $\alpha_{00}$ is due to the residual flux linking the search coil, but not the sample, when the latter is totally superconducting.

Figure 3 (a) and (b) show plots of $K_m$ *vs* $T$ with $H_{z0}$=0.972 amp/cm for the polycrystal and the 6-mm single crystal, respectively. Both of the temperature axes in Fig. 3 are drawn to the same scale. It can be seen that the transitions for the 6-mm single crystal are noticeably broader than those for the 5-mm polycrystal. After obtaining $K_m$ *vs* $T$ curves at two values of $H_{z0}$, specimen Al II was removed from the cryostat for inspection; because of a slight deterioration of the surface, measurements were discontinued on this specimen. Its behavior was intermediate to that observed for specimens Al I and Al III.

Figure 4 (a) and (b) show a plot of the maximum apparent permeability $\tilde{K}_m$ *vs* $I$ for both the 5-mm polycrystal (Al I) and the 6-mm single crystal (Al III). As can be seen from Fig. 4(b), the data taken at the two lowest values of $H_{z0}$ for the 6-mm single crystal show an unexpected crossing of the $\tilde{K}_m$ *vs* $I$ curves. After carefully checking the compensation of the earth's magnetic field, a second run was made which only served to verify the data shown in Fig. 4(b). Since a plot of $I_0$ *vs* $H_{z0}$ for this specimen would obviously depart enormously from a straight line, an $I_g$ for this specimen is undefined. For this reason, the $I_g$ quoted in Table I for aluminum is the value obtained from the 5-mm polycrystal.

## IV. CONCLUSIONS

The paramagnetic effect exists in aluminum. Samples Al II and Al III, although single crystals, were less pure than the polycrystalline sample Al I, as shown by their higher residual resistances. Their paramagnetic behavior did not conform with that observed in other pure superconductors, while the behavior of sample Al I did. We consider therefore that the values of $I_g = 0.3 \pm 0.2$ amp and $\gamma^* = 1.0$, obtained for sample Al I are representative of pure aluminum. These values, together with those of Thompson[5] for indium, indicate that the $I_g$ values do not necessarily occur in multiples of 0.6 amp.

## V. ACKNOWLEDGMENTS

The authors wish to thank the National Science Foundation for supporting this work by a grant. One of us (A.H.F.) wishes to thank the Union Carbide and Carbon Corporation for a fellowship held during the course of this work.

[17] J. R. Clement, in *Temperature; Its Measurement and Control in Science and Industry* (Reinhold Publishing Corporation, New York, 1955), Vol. 2, p. 282.